

# CitDet: A Benchmark Dataset for Citrus Fruit Detection

Jordan A. James<sup>1</sup>, Heather K. Manching<sup>2</sup>, Matthew R. Mattia<sup>3</sup>, Kim D. Bowman<sup>3</sup>,  
Amanda M. Hulse-Kemp<sup>4,2</sup>, and William J. Beksi<sup>1</sup>

**Abstract**—In this letter, we present a new dataset to advance the state of the art in detecting citrus fruit and accurately estimate yield on trees affected by the Huanglongbing (HLB) disease in orchard environments via imaging. Despite the fact that significant progress has been made in solving the fruit detection problem, the lack of publicly available datasets has complicated direct comparison of results. For instance, citrus detection has long been of interest to the agricultural research community, yet there is an absence of work, particularly involving public datasets of citrus affected by HLB. To address this issue, we enhance state-of-the-art object detection methods for use in typical orchard settings. Concretely, we provide high-resolution images of citrus trees located in an area known to be highly affected by HLB, along with high-quality bounding box annotations of citrus fruit. Fruit on both the trees and the ground are labeled to allow for identification of fruit location, which contributes to advancements in yield estimation and potential measure of HLB impact via fruit drop. The dataset consists of over 32,000 bounding box annotations for fruit instances contained in 579 high-resolution images. In summary, our contributions are the following: (i) we introduce a novel dataset along with baseline performance benchmarks on multiple contemporary object detection algorithms, (ii) we show the ability to accurately capture fruit location on tree or on ground, and finally (ii) we present a correlation of our results with yield estimations.

**Index Terms**—Agricultural Automation; Data Sets for Robotic Vision; Deep Learning for Visual Perception

## MULTIMEDIA MATERIAL

The demonstration, dataset, and source code for citrus fruit detection and counting can be found at <https://robotic-vision-lab.github.io/citdet>.

## I. INTRODUCTION

Manuscript received: April 10, 2024; Accepted: September 11, 2024.

This article was recommended for publication by Associate Editor P. V. K. Borges and Editor C. Cadena Lerma upon evaluation of the reviewers' comments. This work was supported by the United States Department of Agriculture (USDA) under USDA-ARS CRIS #6034-21000-018-000-D, #6066-21310-006-000-D, and USDA-ARS Non-Assistance Cooperative Agreement #6066-21310-005-061-S. (Jordan A. James and Heather K. Manching contributed equally to this work.) (Corresponding author: William J. Beksi.)

<sup>1</sup>The authors are with the Department of Computer Science and Engineering, The University of Texas at Arlington, Arlington, TX, USA. Emails: [jaj9608@mavs.uta.edu](mailto:jaj9608@mavs.uta.edu), [william.beksi@uta.edu](mailto:william.beksi@uta.edu).

<sup>2</sup>The author is with the Department of Crop and Soil Sciences, North Carolina State University, Raleigh, NC, USA. Email: [hkmanchi@ncsu.edu](mailto:hkmanchi@ncsu.edu).

<sup>3</sup>The authors are with the Subtropical Insects and Horticulture Research Unit, USDA Agricultural Research Service, Ft. Pierce, FL, USA. Emails: [matthew.mattia@usda.gov](mailto:matthew.mattia@usda.gov), [kim.bowman@usda.gov](mailto:kim.bowman@usda.gov)

<sup>4</sup>The author is with the Genomics and Bioinformatics Research Unit, USDA Agricultural Research Service, Raleigh, NC, USA. Email: [amanda.hulse-kemp@usda.gov](mailto:amanda.hulse-kemp@usda.gov).

Digital Object Identifier (DOI): 10.1109/LRA.2024.3474473



Fig. 1. The **CitDet** dataset contains precise bounding box object annotations for fruit on tree (purple) and fruit on ground (yellow) (top row). It also has images from multiple different tree rows including a large variety of citrus (bottom row).

**F**RUIT detection and counting in orchards are crucial tasks for agricultural automation. They can be used to reduce routine farming and breeding activities as well as provide insightful estimates for harvest and forthcoming growing seasons. Moreover, accurate fruit detection enables the possibility of robotic harvesting, which has the potential to eliminate one of the most labor-intensive processes for growers. Many imaging and sensing technologies have been used for detecting fruit such as hyperspectral [1], laser scanning [2], thermal [3], and RGBD sensors [4, 5], yet the most common technology is the standard RGB camera.

Although conventional RGB cameras are widely accessible, they present several challenges for in-orchard fruit detection such as variation in appearance, irregular lighting, and severe occlusion. Recent works have used deep learning to overcome these difficulties [6]. However, due to the lack of standardized benchmark datasets for agricultural automation, it is difficult to compare these methods with each other. Citrus datasets (e.g., CitrusFarm [7]) have made large amounts of in-orchard citrus images available, yet there still remains a lack of annotated citrus for detection. To tackle this problem we establish a new benchmark dataset, **CitDet** [8, 9], for citrus fruit detection and counting in orchard settings together with a comprehensive analysis of state-of-the-art object detection algorithms, Fig. 1.

Computer vision techniques combined with deep learning are appealing in agricultural automation due to their powerful prediction capabilities and non-invasive nature. Nonetheless, such methods require huge amounts of data to perform with high accuracy. While there exists large datasets (e.g., COCO [10]) that have allowed for the development of new algorithms, many automation tasks require custom datasets to achieve meaningful results. For example, even though COCO contains a class for oranges, an orange detector trained solely from the dataset instances will perform poorly in an orchard setting. This is due to the complex background scenes in COCO, which requires the detector to have more background classification machinery resulting in less orange classification mechanisms [11]. Another reason for the weak performance stems from many instances of oranges with very little or no occlusions in COCO. In orchard fields, oranges can be occluded by other instances of oranges as well as the surrounding foliage. Furthermore, orange instances will not be a large percentage of the image when an entire tree is imaged. These pitfalls highlight the need for unique datasets to carry out fruit detection, yield mapping, and much more.

#### A. Citrus Greening

Citrus greening, also known as Huanglongbing (HLB), is a serious bacterial disease that affects citrus trees and is threatening the existence of the citrus industry, particularly in the southeastern United States [12]. HLB is transmitted by the Asian citrus psyllid, a small insect that feeds on the leaves and shoots of citrus trees. Symptoms of citrus greening include yellowing of the leaves, uneven ripening of the fruit, and reduced fruit size and yield, both in the production of fruit as well as premature fruit loss with fruits dropping to the ground. If left untreated, the disease will ultimately lead to the death of the tree. Currently, there are no effective treatments to cure trees affected by citrus greening. The best way to control the spread of the disease is through a combination of methods such as cultural, biological, chemical, and genetic control along with nutritional management. Nevertheless, none of these countermeasures are foolproof. HLB continues to spread and cause major economic losses for citrus growers.

#### B. Challenges in Detecting Citrus Fruits in Native Orchard Environments

While public datasets for citrus detection exist (e.g., OrangeSORT [13]), to the best of our knowledge **CitDet** is the first dataset to include images of citrus trees affected by HLB, accompanied by paired ground-truth metadata for fruit count. As fruit from an infected tree are likely to be discolored and deformed, labeled examples of affected fruits enhance the robustness of citrus detectors in orchard environments plagued by the disease. Images in contemporary datasets are also low resolution, thus limiting the amount of information to learn and predict from. Finally, the aforementioned datasets only annotate fruit on trees. This can be an issue when training a detector for yield estimation since the model will not learn the difference between dropped fruit and fruit still on the tree, which can be helpful in identifying symptoms of

HLB or secondary fungus associated with post bloom fruit drop. In contrast, **CitDet** aims to boost automation for citrus orchards through high-resolution images of HLB infected citrus trees with accurate annotations for both fruit on tree and fruit on ground. We established an interdisciplinary team to address these challenges, including subject matter experts in the biological system. Our contributions are as follows.

- We captured 579 high-resolution images of citrus trees affected by HLB.
- We provide over 32,000 high-quality annotations of in-orchard citrus, with separate classes of fruit, both on the ground and on the trees.
- We make these images, annotations, and associated fruit count metadata available in multiple public spaces to best serve the broader research communities. The **CitDet** dataset is available through MavMatrix [8] and the USDA Ag Data Commons [9].
- We analyze the baseline performance of detecting citrus fruits using multiple state-of-the-art object detection algorithms.

## II. RELATED WORK

Benchmark datasets provide the means to train and evaluate new algorithms, they are essential to the advancement of deep learning methods. Datasets such as ImageNet [14], Pascal VOC [15], and COCO [10], have publicly released millions of labeled images that contain a variety of classes and objects. Even though these datasets have enabled breakthroughs in image classification, object detection, and object segmentation, there is still a high demand for specialized datasets in agricultural automation. Despite the fact that the number of agricultural datasets continues to grow, there remains a lack of data on fruit affected by common diseases.

#### A. Fruit Detection

Classical methods for fruit detection involve the use of static color thresholds. These methods were enhanced by adding additional sensors such as thermal and near-infrared cameras [20]. In recent years, deep learning-based approaches have shown great promise in the domain of fruit detection. For example, Bargoti and Underwood [16] and Häni et al. [18] used region-based convolutional neural networks to detect fruits in images. Liu et al. [21] utilized a fully-convolutional neural network to segment and detect fruits in a tracking pipeline. DaSNet [22] used atrous spatial pyramid pooling and a gate feature pyramid network to detect and segment in-orchard apples. Fast-FDM [23] leveraged FoveaBox [24] with an EfficientNetV2 [25] backbone to find green apples in the field.

Many works use the YOLO [26] family of object detectors for fruit tracking and yield estimation (e.g., [27, 19, 13]). For instance, Wu et al. [28] modified the YOLOv5 [29] loss function to detect banana bunches at harvest time via extended intersection over union (IoU) [30]. In addition, DeepLabV3+ [31] was utilized to segment banana bunches for counting during sterile bud removal time. Faster R-CNN [32], and the instance segmentation variant Mask R-CNN [33], have

also been successfully employed. Chu *et al.* [34] added a feature suppression network to the end of Mask R-CNN to filter unwanted foliage from the masks. Even though deep learning is advantageous for fruit detection, the task remains challenging due to the unstructured background prevalent in orchards. Tang *et al.* [35] provided an extensive review on strategies involving sensor, image processing, and algorithm optimization for orchard environments.

In-orchard detection of fruits is vital for agricultural tasks including fruit yield estimation and automated picking. For example, Dorj *et al.* [36] leveraged image processing, and the LAB color space, to detect oranges and estimate yield when compared against human observation. Faster R-CNN was used to detect citrus for automated size estimation using drones [37]. Behera *et al.* [38] also utilized Faster R-CNN for detection and yield estimation of various fruits. YOLOv4 [39] was deployed to detect apples and the trunks of trees by Gao *et al.* [40]. The detections are used downstream for apple counting by tracking of the tree trunks in videos. The estimation of tree-level yield by Vijayakumar *et al.* [41] involved the integration of citrus fruit detections from YOLOv3, hyperspectral data, and tree-level traits as inputs for classical machine learning algorithms. Wang *et al.* [42] used YOLOv5 to detect individual lychee and Mask R-CNN to segment the fruit and determine point locations for picking.

### B. Comparison of Datasets

Table I highlights the issues with current fruit detection datasets. Due to the high cost and time involved in labeling data, researchers have opted to use small datasets resulting in a lack of variety. Many works attempt to remedy this by tiling images into smaller sections to artificially increase the overall number of images [16]. Although this technique expands the dataset size, it only shows a small part of the original image and it does not change the total number of object instances. Furthermore, the diversity of the dataset does not increase, which can lead to overfitting when developing machine learning models. While recent research has made available many labeled citrus images [19], the images fail to capture the entire tree and they can suffer from similar overfitting problems.

Another issue is that many of the datasets (e.g., MinneApple [18]) contain fruit on the ground without any labels. This can lead to ambiguity when training a model as it must learn not to detect the fruit on the ground, which can have similar features to that of the fruit on the tree. Other works attempt to solve this issue by treating the unlabeled fruit as a “no object” class and through the introduction of new loss terms

to penalize false positive predictions [19]. Our dataset aims to fix these issues and provide researchers with a means to evaluate and compare their algorithms. To the best of our knowledge, **CitDet** is the *first* fruit detection dataset to provide full-resolution images with annotations for both fruit on trees and on the ground. It is the *only* citrus dataset to contain images of entire citrus trees. In addition, we include a variety of citrus tree species imaged at different stages of maturity under varying illumination conditions to avoid overfitting.

### III. IMAGE COLLECTION

**CitDet** is composed of images captured at the USDA Agricultural Research Service Subtropical Insects and Horticulture Research Unit in Fort Pierce, Florida, between October 2021 and October 2022. The orchard contains a large assortment of citrus tree species and is used for genomics and phenotyping research involving citrus infected with HLB. We collected 579 images from different sections of the orchard using Field Book [43] on Android tablets. While imaging the plants, we faced the camera in a portrait orientation directly centered on the tree of interest. All images were taken at the edge of the soil in the tree row to simulate a ground-based robot imaging the tree while moving between two rows of trees.

Data was collected over the course of one year to allow the fruit to be imaged at different stages of the ripening cycle during citrus production from October to March. Due to the nature of HLB and the mixture of fruit maturity, **CitDet** contains fruit of different colors and sizes. All trees were imaged from both the sunny and shady sides of the tree row and imaging was done over multiple days to account for variations in lighting and weather conditions. The imaged trees consist of 60 different varieties of citrus, representing 8 different species of citrus and other related genera. All images include a timestamp, tree ID, and the side of the tree imaged in the file name.

The dataset was split into 80% for the training set and 20% for the test set. Images included in the test set were chosen to cover a variety of citrus tree species and cultivars with fruits of varied color, shape, and size. Specifically, images in the test set contain unique views of fruit imaged from both shady and sunny sides of the tree at varied times of the day. Additionally, we collected observed yield estimates for 187 randomly selected trees by counting the number of fruit per tree prior to imaging. Out of the acquired images 130 were not included in the final dataset. This was done to avoid blurry and background fruit, which can be ambiguous to annotate. Succeeding work may consider coarse annotations for fruit in the background. Since we do not include a benchmark or

TABLE I  
COMPARISON OF FRUIT DETECTION DATASETS

Fruit Detection	Fruit	# of Images	# of Annotations	# of Classes	Resolution	Ground Truth
Bargoti <i>et al.</i> [16]	Apple	841	5,765	1	308 × 202	Circles
Stein <i>et al.</i> [17]	Mango	1,404	7,065	1	500 × 500	Circles
Häni <i>et al.</i> [18]	Apple	1,001	41,325	1	720 × 1,280	Polygons
Hou <i>et al.</i> [19]	Citrus	4,855	17,567	1	1,280 × 720	Boxes
<b>CitDet</b>	Citrus	579	44,233	2	2,448 × 3264	Boxes
<b>CitDet (Tiled)</b>	Citrus	5,211	46,630	2	816 × 1,088	Boxes

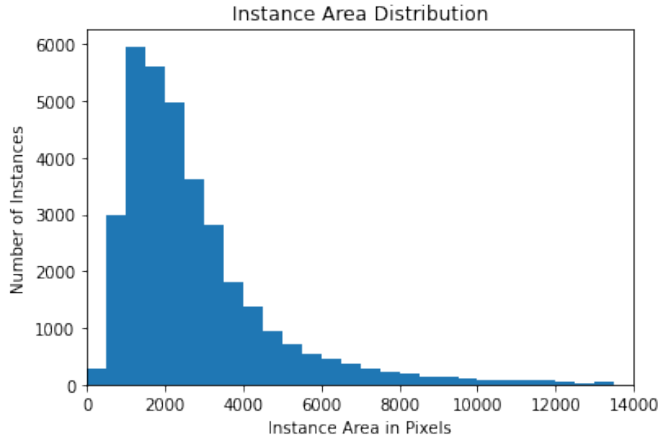


Fig. 2. The area distribution of the objects in **CitDet**. The dataset is mainly comprised of small object instances with an area of less than  $50^2$  pixels.

dataset for tracking, we use the predicted detections from the model as yield estimation and validate against the ground truth.

#### IV. IMAGE ANNOTATION

To construct **CitDet**, we followed standard annotation methods found in other benchmark object detection datasets. The Roboflow [44] annotation tool was used to label the image data with bounding boxes. Specifically, we labeled all visible fruit in the foreground regardless of occlusions, while fruit in the background was only labeled for instances with no occlusions. We do not provide any annotations for fruits that are fully occluded and thus not visible. Each of the labeled objects in an image are classified as either fruit on tree or fruit on ground.

**CitDet** is unique for fruit detection in that we provide labels for fruit that has already fallen. This allows detection methods to accurately identify fruit that contributes to the overall fruit yield. Since a single image can contain a large number of object instances and a heavy amount of occlusions, labeling images is a time-consuming task. For instance, annotating a single image can take up to half an hour. Therefore, the task of instance labeling was split among several internal volunteers and each image was assigned to only one volunteer to annotate. After labeling, each image was then reviewed by a single expert to validate the quality of the annotations.

#### V. DATASET STATISTICS

Popular image datasets (e.g., ImageNet, Pascal VOC, and COCO) focus on detecting many categories of objects in a multitude of natural settings. In each of these datasets, most object instances tend to occupy over 10% of the image area. As a result, the majority of images contain few object instances per image. In comparison, **CitDet** provides a unique collection of small, highly-cluttered objects under various levels of occlusion.

Since the **CitDet** dataset does not contain many different categories, it is comparable to the Caltech Pedestrian Detection [45], KITTI [46], and MinneApple datasets where each dataset focuses on providing many labeled object instances per category. Specifically, our dataset is similar to MinneApple

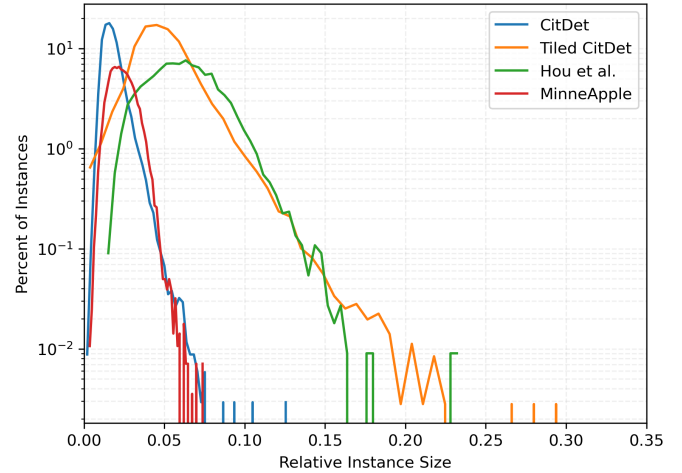


Fig. 3. A comparison of the relative instance size (square root of instance area divided by total image area) between fruit detection datasets.

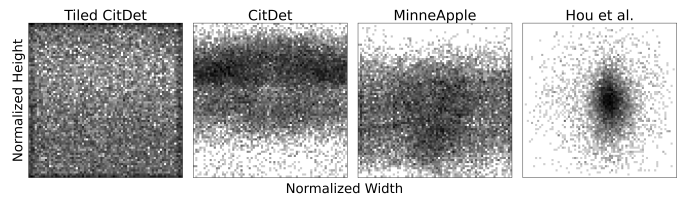


Fig. 4. The distribution of object centers in normalized image coordinates for four datasets. **CitDet** exhibits the greatest spatial diversity among the citrus datasets, with the tiled version exhibiting greater complexity than all the other fruit datasets.

as both provide a large number of annotations for fruit in an orchard setting. The main difference is that our dataset provides annotations of fallen fruit as well as fruit still on the tree. **CitDet** allows models to automatically distinguish between dropped and non-dropped fruit, enabling accurate yield estimation without any additional postprocessing.

**CitDet** also provides a challenge for state-of-the-art detection algorithms due to the small average size of the object instances. Small objects are generally harder to detect and require specialized network structures. In ImageNet, Pascal VOC, and COCO, only 50% of the objects occupy less than 10% of an image while the remaining 50% of the objects occupy between 10% and 100% of an image. Conversely, over 90% of the objects in **CitDet** take up less than 10% of an image. As displayed in Fig. 2, the average object in our dataset is only  $50 \times 50$  pixels, which corresponds to less than 0.1% of an image. In contrast, objects in MinneApple occupy around 0.17% of an image. Although the average object in **CitDet** is smaller, the distribution of relative instance size is similar to MinneApple as shown in Fig. 3. The high resolution of **CitDet** allows for preprocessing techniques (e.g., tiling) to shift the relative distribution and increase spatial complexity. This increases the versatility of the dataset as highlighted in Fig. 4. Another key difference between **CitDet** and MinneApple is the format of the object annotations, bounding boxes versus polygons, respectively.

## VI. ALGORITHMIC ANALYSIS

We applied multiple state-of-the-art object detection algorithms on **CitDet** to establish a baseline for future work. For all the experiments, we used the same 460 images from our dataset for training while the remaining 119 images were utilized as the test set. We divided the experiments into two tasks: (i) detection on the whole (full-resolution) image dataset, and (ii) detection on the tiled image dataset. The tiled image dataset was created by splitting every image into 9 separate images using a  $3 \times 3$  cropping method. For any bounding box split by the cropping, a bounding box for each portion of the object was created in each of the new images resulting in slightly more object instances. The resulting dataset contains 5,211 images at a resolution of  $816 \times 1088$ .

### A. Fruit Detection

In all the experiments, the models were trained using an NVIDIA Tesla T4 GPU and restricted to similar levels of compute power. Every algorithm tested used pretrained COCO weights for initialization and they were fine-tuned for 50 epochs on the tiled dataset. The models tested on the whole image dataset used pretrained weights from the tiled dataset and they were fine-tuned for 50 epochs on resized images of  $704 \times 704$  resolution. We evaluated each of the algorithms on the test set and reported the average performance for each class as well as the mean average performance of all classes.

**Detection evaluation metrics:** We followed the established evaluation protocols used by other benchmark object detection datasets (e.g., [15, 10, 18]). For a single class, we reported the average precision (AP) as the main evaluation metric. We also recorded the mean AP (mAP) of all classes. For the AP of a class we used an IoU threshold of 0.5, increased it in intervals of 0.05 up to 0.95, and reported the mean of the AP at each threshold. The AP at thresholds of 0.5 and 0.75, as well as the AP for small ( $AP_S$ ), medium ( $AP_M$ ), and large ( $AP_L$ ) objects, are also provided.

**Faster R-CNN:** Faster R-CNN utilizes a ResNet-50 [47] backbone along with a feature pyramid network. The implementation makes use of region proposal networks as the head of the detection network and two branches for predicting the class and bounding boxes. We used a k-means clustering algorithm with IoU and ground-truth labels in the training dataset to determine the anchor box sizes. All the other optimization parameters were the same as the original paper.

**YOLOv5:** The implementation of YOLOv5 is provided by Ultralytics. YOLOv5 uses a different architecture compared to previous versions of YOLO. In particular, it has a cross stage partial backbone architecture, which is a combination of two types of convolutional layers: depth-wise convolution and point-wise convolution. The architecture not only reduces the computational and memory requirements of the model, but also improves the overall accuracy.

**YOLOv7:** YOLOv7 [48] improves upon real-time object detection performance by designing a trainable “bag-of-freebies” set of methods. The detector addresses two new issues in object detection evolution by proposing the “extend” and “compound scaling” techniques. The proposed methods

TABLE II  
WHOLE IMAGE DATASET RESULTS

Model	# of Params	AP	AP <sub>50</sub>	AP <sub>S</sub>	AP <sub>M</sub>	AP <sub>L</sub>
Faster R-CNN	41.3 M	22.0	51.5	<b>21.8</b>	<b>44.2</b>	-
YOLOv5	21.1 M	34.8	70.0	9.0	36.9	46.3
YOLOv7	36.5 M	<b>40.6</b>	<b>77.9</b>	12.3	42.6	<b>49.7</b>

TABLE III  
TILED IMAGE DATASET RESULTS

Model	# of Params	AP	AP <sub>50</sub>	AP <sub>S</sub>	AP <sub>M</sub>	AP <sub>L</sub>
YOLOS	30.9 M	32.4	70.7	10.3	35.8	47.9
DETR	41.3 M	35.0	72.8	9.8	38.7	49.8
Faster R-CNN	41.3 M	37.2	76.0	<b>24.1</b>	44.4	45.9
YOLOv5	21.1 M	44.9	81.9	18.2	49.2	50.6
YOLOv7	36.5 M	<b>45.5</b>	<b>83.1</b>	19.2	<b>49.4</b>	<b>52.1</b>

reduce the number of parameters and the amount of computation by approximately 40% and 50%, respectively. They also result in faster inference speed and higher detection accuracy.

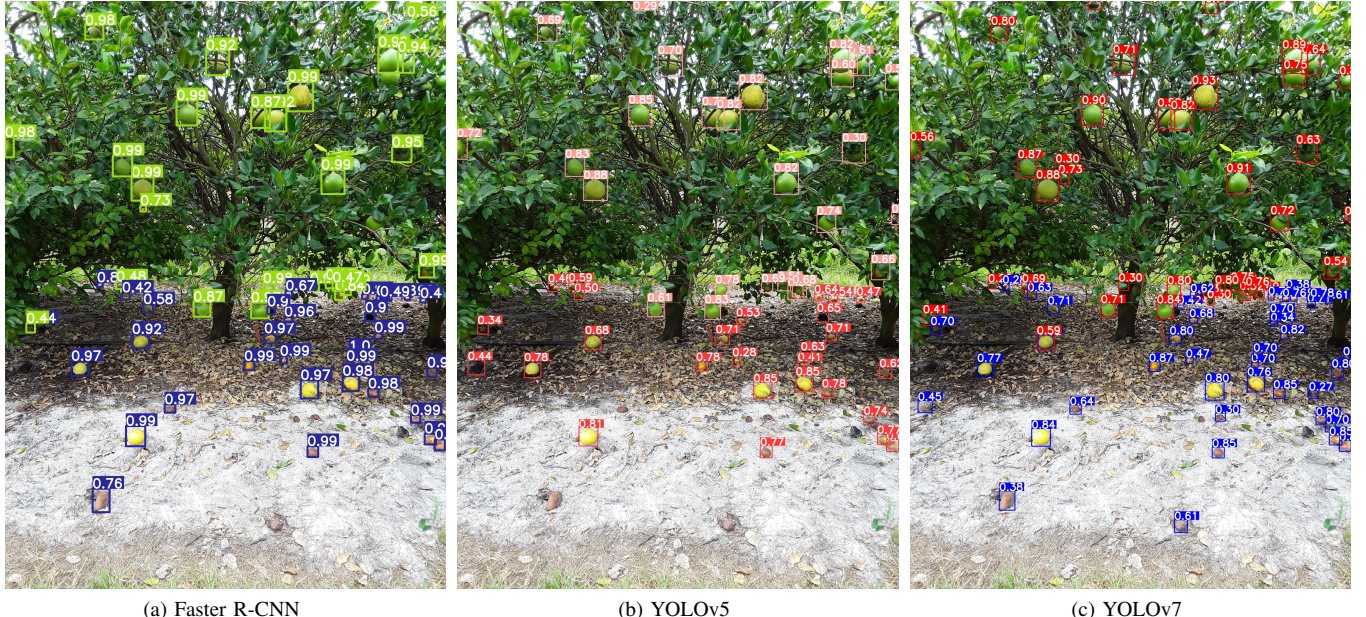
**DETR:** The DETR [49] model for object detection was introduced by Facebook Artificial Intelligence Research. It uses a ResNet-50 backbone to embed image features as input to a transformer encoder-decoder. The architecture utilizes a standard transformer encoder-decoder with the addition of object query tokens passed to the decoder. The network is trained using a bipartite matching loss, thus removing the need for non-maximum suppression. We used sine positional embeddings for both the encoder and decoder.

**YOLOS:** You Only Look at One Sequence (YOLOS) [50] leverages a vanilla vision transformer (ViT) [51] encoder with minimal multilayer perceptron heads for object detection. The YOLOS ViT architecture is the same as DeiT [52] and includes a distillation token for training. Images are represented by a sequence of  $16 \times 16$  patches. The patches are projected and inputted as tokens to the transformer encoder along with positional embedding tokens. YOLOS feeds detection token inputs to an encoder, which are then decoded by the head to predict the bounding box and class. Similar to DETR, the network is trained using a bipartite matching loss. We utilized sine positional embeddings for the implementation tested.

### B. Discussion

Contrary to other fruit detection works, we found that processing the image in a tiled manner performs better than detectors that operate on the full image. We hypothesize that there are two primary factors for this. The first factor is the difference between the tiling methods used. For example, in the Bargoti and Underwood [16] model, training images are split into overlapping chunks, which requires the filtering of overlapping bounding boxes. Our tiling method does not have any overlap. Instead, we process the bounding boxes on the edges of the fruits before training and therefore do not require the filtering step at the end. The second factor contributing to the improved performance of the tiled versions is the ability to preserve information when resizing the image for the model.

In comparing the state-of-the-art object detection algorithms, we found that YOLOv7 outperformed all the other algorithms on both the whole and tiled images. However,

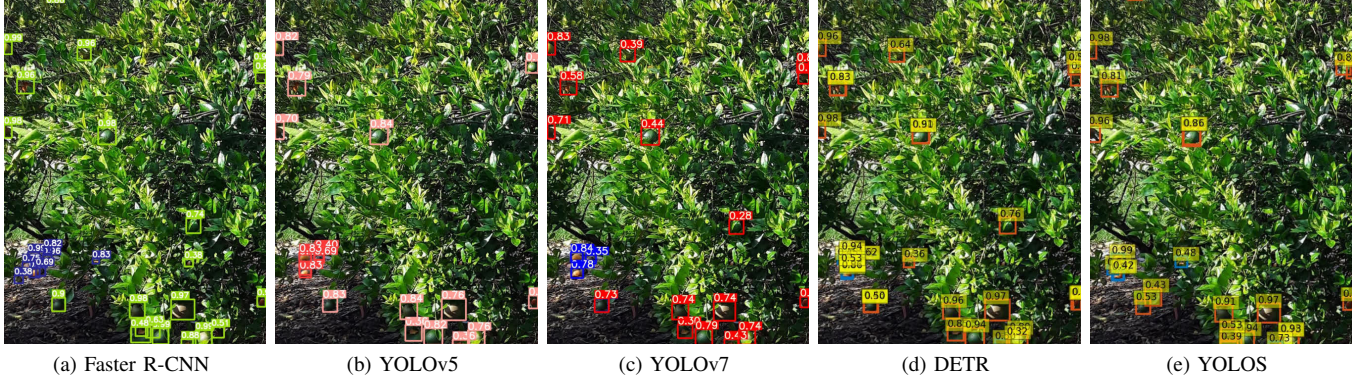


(a) Faster R-CNN

(b) YOLOv5

(c) YOLOv7

Fig. 5. Visualizations of the qualitative results for each network on the same full validation image. The bounding box annotations are colored based on the predicted class label with differing color schemes for each network.



(a) Faster R-CNN

(b) YOLOv5

(c) YOLOv7

(d) DETR

(e) YOLOS

Fig. 6. Visualizations of the qualitative results for each network on the same tiled validation image. The bounding box annotations are colored based on the predicted class label with differing color schemes for each network.

Faster R-CNN performed the best for small objects on both image types. The results in Tables II and III suggest that the YOLO architectures benefit more from transfer learning on high-resolution images when compared to Faster R-CNN. All the networks demonstrate the capability to distinguish between fruit yield and drop even in ambiguous cases such as in Fig. 5 and Fig. 6. We observed that all the methods struggled to accurately detect small object instances. We note that standard convolutional approaches performed better than transformers for small object detection. Nonetheless, future research is needed to accurately detect small and medium sized objects for all methods. Our findings confirm previous works (e.g., [53, 18]), which found that object size is one of the main determinants of error in object detection.

#### C. Yield Estimation

Yield estimation is performed at the tree level to provide higher-resolution information for downstream tasks such as

phenomic selection for citrus breeding. Additional analysis at the row level can be performed by aggregation of the tree-level estimates. To further validate the detection results, we used a detection only based yield estimation method for each tree and compared it with the ground-truth estimates as currently used in breeding programs for observed fruit yield values. In this experiment, we acquired front and back images of 187 trees before harvest. A YOLOv7 model was trained on a subset of **CitDet**, which excluded images of trees in the yield estimation test set. Breeding program measured fruit yield estimates for each tree were recorded and used as the ground-truth yield values.

For all the experiments we consider only the fruit on the trees for prediction of the fruit yield. We evaluated the per-tree yield prediction correlation with the ground-truth estimates

TABLE IV  
TREE YIELD CORRELATION

Method	Front R <sup>2</sup>	Back R <sup>2</sup>	Front+Back R <sup>2</sup>
detect-count	0.584	0.635	0.754
filter-detect-count	0.603	0.677	0.793

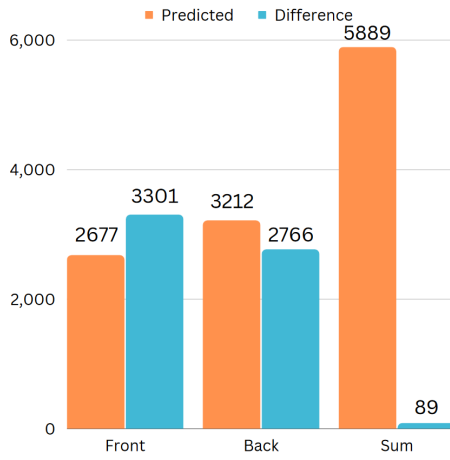


Fig. 7. The total predicted yield and the difference of actual and predicted yield for 187 sample citrus trees of varying species and maturity obtained using the filter-detect-count method. We used infield hand counts acquired by technicians as the ground-truth yield.

using the square of the Pearson correlation coefficient,

$$R^2 = \left( \frac{\sum_{i=1}^n (x_i - \bar{x})(y_i - \bar{y})}{\sqrt{\sum_{i=1}^n (x_i - \bar{x})^2} \sqrt{\sum_{i=1}^n (y_i - \bar{y})^2}} \right)^2, \quad (1)$$

where  $n$  is the total number of trees in the experiment,  $x$  and  $y$  are the predicted and ground-truth yield estimates, and  $\bar{x}$  and  $\bar{y}$  are the mean of the predicted and ground-truth yield estimates. Two simple yield estimation methods were compared: detect-count and filter-detect-count. The  $R^2$  values are reported in Table IV.

The first method for yield estimation, detect-count, simply detects the fruit in an image and estimates the counts of fruit labeled as fruit on the tree with a confidence of at least 0.3. Detection is applied to both the front and back images, and yield is estimated separately for each. We made the assumption that due to the high amount of foliage on the trees, fruits that are visible in one view will be occluded in the other view. As such, the sum of the predicted counts for each view of the tree are used as the predicted fruit yield.

An analysis of large prediction errors showed that many images contained parts of neighboring trees in the image, which attributed to higher fruit counts. The second method, filter-detect-count, aims to address this issue by using a two-stage detection approach to filter out neighboring trees. The first stage uses a separate model to detect all trees and their canopies. Then, the central most detection is taken as input to the second stage and passed to a YOLO model for fruit detection. The improved method correctly predicted four out of the five top-producing trees with an error of only -1.49% on the total yield estimation of the orchard as shown in Fig. 7.

## VII. CONCLUSION AND FUTURE WORK

In this work we introduced **CitDet**, a new dataset for citrus detection in orchards prone to citrus greening. By distinguishing between fruit on the ground and fruit on the trees, we showed that it is possible to identify fruit that contributes to yield via a single model. With this annotated collection of citrus, we aim to increase the comparability of fruit detection algorithms and advance research on this topic. Importantly, the metadata and associated tree-level yield estimates are included to serve as a ground-truth metric.

Detectors trained on **CitDet** can be applied for citrus tracking and yield estimation, size estimation, and automated fruit picking in follow-up studies. The results of the object detection benchmarks indicate that **CitDet** is challenging for modern detectors and there are many opportunities for subsequent research and improvement. In particular, future work is necessary to improve the accuracy of detectors on small objects in cluttered environments and the inclusion of biological ground-truth data will allow for further analysis.

## ACKNOWLEDGMENTS

The authors thank members of the Hulse-Kemp Lab including Dr. Keo Corak, Dr. Emily Delorean, Ashley Schoonmaker, Grant Billings, and Cassie Newman for assistance in image annotation and USDA-ARS USHRL technicians Jefferson Shaw and Darren Cole for assistance in image collection.

## REFERENCES

- [1] Y. Ding, W. S. Lee, and M. Li, "Feature extraction of hyperspectral images for detecting immature green citrus fruit," *Frontiers of Agricultural Science and Engineering*, vol. 5, no. 4, pp. 475–484, 2018.
- [2] J. Gené-Mola, E. Gregorio, J. Guevara, F. Auat, R. Sanz-Cortiella, A. Escolà, J. Llorens, J.-R. Morros, J. Ruiz-Hidalgo, V. Vilaplana, and J. R. Rosell-Polo, "Fruit detection in an apple orchard using a mobile terrestrial laser scanner," *Biosystems Engineering*, vol. 187, pp. 171–184, 2019.
- [3] H. Gan, W. S. Lee, V. Alchanatis, and A. Abd-Elrahman, "Active thermal imaging for immature citrus fruit detection," *Biosystems Engineering*, vol. 198, pp. 291–303, 2020.
- [4] Z. Wang, K. B. Walsh, and B. Verma, "On-tree mango fruit size estimation using rgb-d images," *Sensors*, vol. 17, no. 12, p. 2738, 2017.
- [5] G. Lin, Y. Tang, X. Zou, J. Li, and J. Xiong, "In-field citrus detection and localisation based on rgb-d image analysis," *Biosystems Engineering*, vol. 186, pp. 34–44, 2019.
- [6] A. Koirala, K. B. Walsh, Z. Wang, and C. McCarthy, "Deep learning - method overview and review of use for fruit detection and yield estimation," *Computers and Electronics in Agriculture*, vol. 162, pp. 219–234, 2019.
- [7] H. Teng, Y. Wang, X. Song, and K. Karydis, "Multimodal dataset for localization, mapping and crop monitoring in citrus tree farms," in *International Symposium on Visual Computing*. Springer, 2023, pp. 571–582.
- [8] J. A. James, H. K. Manching, M. R. Mattia, K. D. Bowman, A. M. Hulse-Kemp, and W. J. Beksi, "CitDet," 2024. [Online]. Available: <https://doi.org/10.32855/dataset.2024.05.005>
- [9] ———, "CitDet," 2024. [Online]. Available: <https://doi.org/10.15482/USDA.ADC/1529611>
- [10] T.-Y. Lin, M. Maire, S. Belongie, J. Hays, P. Perona, D. Ramanan, P. Dollár, and C. L. Zitnick, "Microsoft coco: Common objects in context," in *Proceedings of the European Conference on Computer Vision*. Springer, 2014, pp. 740–755.
- [11] D. Miller, G. Goode, C. Bennie, P. Moghadam, and R. Jurdak, "Why object detectors fail: Investigating the influence of the dataset," in *Proceedings of the IEEE/CVF Conference on Computer Vision and Pattern Recognition*, 2022, pp. 4823–4830.

[12] S. Alvarez, E. Rohrig, D. Solís, and M. H. Thomas, "Citrus greening disease (huanglongbing) in florida: Economic impact, management and the potential for biological control," *Agricultural Research*, vol. 5, pp. 109–118, 2016.

[13] W. Zhang, J. Wang, Y. Liu, K. Chen, H. Li, Y. Duan, W. Wu, Y. Shi, and W. Guo, "Deep-learning-based in-field citrus fruit detection and tracking," *Horticulture Research*, vol. 9, 2022.

[14] J. Deng, W. Dong, R. Socher, L.-J. Li, K. Li, and L. Fei-Fei, "Imagenet: A large-scale hierarchical image database," in *Proceedings of the IEEE/CVF Conference on Computer Vision and Pattern Recognition*, 2009, pp. 248–255.

[15] M. Everingham, L. Van Gool, C. K. Williams, J. Winn, and A. Zisserman, "The pascal visual object classes (voc) challenge," *International Journal of Computer Vision*, vol. 88, pp. 303–338, 2010.

[16] S. Bargoti and J. Underwood, "Deep fruit detection in orchards," in *Proceedings of the IEEE International Conference on Robotics and Automation*, 2017, pp. 3626–3633.

[17] M. Stein, S. Bargoti, and J. Underwood, "Image based mango fruit detection, localisation and yield estimation using multiple view geometry," *Sensors*, vol. 16, no. 11, p. 1915, 2016.

[18] N. Häni, P. Roy, and V. Isler, "Minneapple: A benchmark dataset for apple detection and segmentation," *IEEE Robotics and Automation Letters*, vol. 5, no. 2, pp. 852–858, 2020.

[19] C. Hou, X. Zhang, Y. Tang, J. Zhuang, Z. Tan, H. Huang, W. Chen, S. Wei, Y. He, and S. Luo, "Detection and localization of citrus fruit based on improved you only look once v5s and binocular vision in the orchard," *Frontiers in Plant Science*, vol. 13, 2022.

[20] A. Gongal, S. Amaty, M. Karkee, Q. Zhang, and K. Lewis, "Sensors and systems for fruit detection and localization: A review," *Computers and Electronics in Agriculture*, vol. 116, pp. 8–19, 2015.

[21] X. Liu, S. W. Chen, S. Aditya, N. Sivakumar, S. Dcunha, C. Qu, C. J. Taylor, J. Das, and V. Kumar, "Robust fruit counting: Combining deep learning, tracking, and structure from motion," in *Proceedings of the IEEE/RSJ International Conference on Intelligent Robots and Systems*, 2018, pp. 1045–1052.

[22] H. Kang and C. Chen, "Fruit detection and segmentation for apple harvesting using visual sensor in orchards," *Sensors*, vol. 19, no. 20, p. 4599, 2019.

[23] W. Jia, Z. Wang, Z. Zhang, X. Yang, S. Hou, and Y. Zheng, "A fast and efficient green apple object detection model based on foveabox," *Journal of King Saud University-Computer and Information Sciences*, vol. 34, no. 8, pp. 5156–5169, 2022.

[24] T. Kong, F. Sun, H. Liu, Y. Jiang, L. Li, and J. Shi, "Foveabox: Beyond anchor-based object detection," *IEEE Transactions on Image Processing*, vol. 29, pp. 7389–7398, 2020.

[25] M. Tan and Q. Le, "Efficientnetv2: Smaller models and faster training," in *International Conference on Machine Learning*. PMLR, 2021, pp. 10096–10 106.

[26] J. Redmon, S. Divvala, R. Girshick, and A. Farhadi, "You only look once: Unified, real-time object detection," in *Proceedings of the IEEE/CVF Conference on Computer Vision and Pattern Recognition*, 2016, pp. 779–788.

[27] H. Mirhaji, M. Soleimani, A. Asakereh, and S. A. Mehdizadeh, "Fruit detection and load estimation of an orange orchard using the yolo models through simple approaches in different imaging and illumination conditions," *Computers and Electronics in Agriculture*, vol. 191, p. 106533, 2021.

[28] F. Wu, Z. Yang, X. Mo, Z. Wu, W. Tang, J. Duan, and X. Zou, "Detection and counting of banana bunches by integrating deep learning and classic image-processing algorithms," *Computers and Electronics in Agriculture*, vol. 209, p. 107827, 2023.

[29] G. Jocher, "YOLOv5 by ultralytics," 2020. [Online]. Available: <https://github.com/ultralytics/yolov5>

[30] H. Peng and S. Yu, "A systematic iou-related method: Beyond simplified regression for better localization," *IEEE Transactions on Image Processing*, vol. 30, pp. 5032–5044, 2021.

[31] L.-C. Chen, Y. Zhu, G. Papandreou, F. Schroff, and H. Adam, "Encoder-decoder with atrous separable convolution for semantic image segmentation," in *Proceedings of the European Conference on Computer Vision*, 2018, pp. 801–818.

[32] S. Ren, K. He, R. Girshick, and J. Sun, "Faster r-cnn: Towards real-time object detection with region proposal networks," in *Proceedings of the Advances in Neural Information Processing Systems*, vol. 28, 2015.

[33] K. He, G. Gkioxari, P. Dollár, and R. Girshick, "Mask r-cnn," in *Proceedings of the IEEE/CVF Conference on Computer Vision and Pattern Recognition*, 2017, pp. 2961–2969.

[34] P. Chu, Z. Li, K. Lammers, R. Lu, and X. Liu, "Deep learning-based apple detection using a suppression mask r-cnn," *Pattern Recognition Letters*, vol. 147, pp. 206–211, 2021.

[35] Y. Tang, J. Qiu, Y. Zhang, D. Wu, Y. Cao, K. Zhao, and L. Zhu, "Optimization strategies of fruit detection to overcome the challenge of unstructured background in field orchard environment: A review," *Precision Agriculture*, pp. 1–37, 2023.

[36] U.-O. Dorj, M. Lee, and S.-s. Yun, "An yield estimation in citrus orchards via fruit detection and counting using image processing," *Computers and Electronics in Agriculture*, vol. 140, pp. 103–112, 2017.

[37] O. Apolo-Apolo, J. Martínez-Guante, G. Egea, P. Raja, and M. Pérez-Ruiz, "Deep learning techniques for estimation of the yield and size of citrus fruits using a uav," *European Journal of Agronomy*, vol. 115, p. 126030, 2020.

[38] S. K. Behera, A. K. Rath, and P. K. Sethy, "Fruits yield estimation using raster r-cnn with miou," *Multimedia Tools and Applications*, vol. 80, pp. 19 043–19 056, 2021.

[39] A. Bochkovskiy, C.-Y. Wang, and H.-Y. M. Liao, "Yolov4: Optimal speed and accuracy of object detection," *arXiv preprint arXiv:2004.10934*, 2020.

[40] F. Gao, W. Fang, X. Sun, Z. Wu, G. Zhao, G. Li, R. Li, L. Fu, and Q. Zhang, "A novel apple fruit detection and counting methodology based on deep learning and trunk tracking in modern orchard," *Computers and Electronics in Agriculture*, vol. 197, p. 107000, 2022.

[41] V. Vijayakumar, Y. Ampatzidis, and L. Costa, "Tree-level citrus yield prediction utilizing ground and aerial machine vision and machine learning," *Smart Agricultural Technology*, vol. 3, p. 100077, 2023.

[42] H. Wang, Y. Lin, X. Xu, Z. Chen, Z. Wu, and Y. Tang, "A study on long-close distance coordination control strategy for litchi picking," *Agronomy*, vol. 12, no. 7, p. 1520, 2022.

[43] T. W. Rife and J. A. Poland, "Field book: An open-source application for field data collection on android," *Crop Science*, vol. 54, no. 4, pp. 1624–1627, 2014.

[44] B. Dwyer, J. Nelson, and J. Solawetz, "Roboflow (version 1.0)," 2022. [Online]. Available: <https://roboflow.com>

[45] P. Dollár, C. Wojek, B. Schiele, and P. Perona, "Pedestrian detection: A benchmark," in *Proceedings of the IEEE/CVF Conference on Computer Vision and Pattern Recognition*, 2009, pp. 304–311.

[46] A. Geiger, P. Lenz, C. Stiller, and R. Urtasun, "Vision meets robotics: The kitti dataset," *The International Journal of Robotics Research*, vol. 32, no. 11, pp. 1231–1237, 2013.

[47] K. He, X. Zhang, S. Ren, and J. Sun, "Deep residual learning for image recognition," in *Proceedings of the IEEE/CVF Conference on Computer Vision and Pattern Recognition*, 2016, pp. 770–778.

[48] C.-Y. Wang, A. Bochkovskiy, and H.-Y. M. Liao, "Yolov7: Trainable bag-of-freebies sets new state-of-the-art for real-time object detectors," in *Proceedings of the IEEE/CVF Conference on Computer Vision and Pattern Recognition*, 2023, pp. 7464–7475.

[49] N. Carion, F. Massa, G. Synnaeve, N. Usunier, A. Kirillov, and S. Zagoruyko, "End-to-end object detection with transformers," in *Proceedings of the European Conference on Computer Vision*. Springer, 2020, pp. 213–229.

[50] Y. Fang, B. Liao, X. Wang, J. Fang, J. Qi, R. Wu, J. Niu, and W. Liu, "You only look at one sequence: Rethinking transformer in vision through object detection," in *Proceedings of the Advances in Neural Information Processing Systems*, vol. 34, 2021, pp. 26 183–26 197.

[51] A. Dosovitskiy, L. Beyer, A. Kolesnikov, D. Weissenborn, X. Zhai, T. Unterthiner, M. Dehghani, M. Minderer, G. Heigold, S. Gelly, J. Uszkoreit, and N. Houlsby, "An image is worth 16x16 words: Transformers for image recognition at scale," in *Proceedings of the International Conference on Learning Representations*, vol. 406, 2021, p. 407.

[52] H. Touvron, M. Cord, M. Douze, F. Massa, A. Sablayrolles, and H. Jégou, "Training data-efficient image transformers & distillation through attention," in *Proceedings of the International Conference on Machine Learning*. PMLR, 2021, pp. 10 347–10 357.

[53] D. Hoiem, Y. Chodpathumwan, and Q. Dai, "Diagnosing error in object detectors," in *Proceedings of the European Conference on Computer Vision*, 2012, pp. 340–353.